Anal. Bioanal. Electrochem., Vol. 17, No. 9, 2025, 824-840
https://www.doi.org/10.22034/abec.2025.739011

Analytical & Bioanalytical Electrochemistry

Full Paper

Mechanistic Study and Computational Analysis of the Electrochemical Oxidation of Caffeic Acid in the Presence of Different Nucleophiles

Hadi Beiginejad,* and Seyed Abdollah Shojaeie

Department of Applied Chemistry, Faculty of Science, Malayer University, Malayer 65174, Iran

*Corresponding Author, Tel.: +988132355404
E-Mail: h.beiginejad@malayeru.ac.ir

Received: 5 October 2025 / Received in revised form: 20 December 2025 / Accepted: 21 December 2025 / Published online: 31 December 2025

Abstract- The electrochemical oxidation of caffeic acid in the presence of *p*-toluenesulfinic acid, methyl-Meldrum's acid, phenyl-Meldrum's acid, barbituric acid, and Meldrum's acid as nucleophiles was investigated using experimental and theoretical approaches. Experimental studies were conducted using cyclic voltammetry, linear sweep voltammetry, and controlled-potential coulometry. Theoretical calculations were performed using density functional theory (DFT) at the BP86 level with the 6-31G (d,p) basis set. The results indicate that the electrochemical oxidation of caffeic acid in the presence of *p*-toluenesulfinic acid, methyl-Meldrum's acid, and phenyl-Meldrum's acid follows an *EC* mechanism, where *E* denotes an electrochemical step and *C* represents a subsequent chemical reaction. In contrast, the oxidation of caffeic acid in the presence of barbituric acid and Meldrum's acid proceeds via an *ECEC* mechanism. To elucidate the origin of these mechanistic differences, computational studies were conducted. The results obtained using a general thermodynamic cycle demonstrate that the reaction pathway depends on the Gibbs free energy change (ΔG) of the electrochemical oxidation step, which determines whether the species generated at the electrode surface undergoes subsequent electrochemical or chemical reactions.

Keywords- Electrochemical oxidation; Controlled-potential coulometry; Caffeic acid; ΔG_{tot}

1. INTRODUCTION

Electrochemistry has been widely employed to synthesize organic compounds [1-5]. The electrochemical oxidation of electroactive compounds in the presence of nucleophiles can proceed through various mechanistic pathways, including *EC*, *ECE*, *ECEC*, *ECECE*, and etc.

[6-10]. (where *E* represents an electrochemical reaction and *C* represents a subsequent chemical reaction). Different electrophiles in the presence of similar nucleophiles can exhibit either analogous or distinct mechanisms. For example, the electrochemical oxidation mechanism of 1-[4-(4- hydroxyphenyl)piperazin-1-yl]ethanone in the presence of 2-mercaptobenzothiazole is *ECECEC* [11], whereas the mechanism for 3-methylcatechol under the same conditions is *EC* [12]. This is in contrast to the electrochemical oxidation both species 1-[4-(4-hydroxyphenyl)piperazin-1-yl]ethanone and 3-methylcatechol in the presence of p-toluenesulfinic acid, which have a similar mechanism (*EC*) [13,14]. The electrochemical oxidation of dihydroxybenzenes in the presence of Meldrum's acid derivatives has been investigated. It was reported that the electrochemical oxidation of hydroquinone with methyl-Meldrum's acid follows an *ECE* mechanism [15], whereas the mechanism for catechol under the same conditions is *EC* [16]. Computational studies were employed to analyze the mechanisms of these electrochemical oxidations, revealing that the total Gibbs free energy change (ΔG_{tot}) of the oxidation of intermediates and products is one of the most parameters influencing the reaction mechanisms. Depending on the ΔG of the electrochemical oxidation, the products formed on the electrode surface will participate in the electrochemical or chemical following reactions [17-20]. In the present research, the electrochemical oxidation of caffeic acid in the presence of *p*-toluenesulfinic acid, methyl-Meldrum's acid, phenyl-Meldrum's acid, barbituric acid, and Meldrum's acid were studied both experimentally and theoretically. Cyclic voltammetry, linear sweep voltammetry, and controlled-potential coulometry were used to obtain the experimental results. Based on previous experience, the theoretical results were calculated at DFT (BP86) level of theory and 6–31G (p,d) basis set according to the Born-Haber cycle [15,20,29]. It was found that caffeic acid oxidized to it's correspond *o*-benzoquinone (**1ox**), then electrochemically generated **1ox** reacts with nucleophiles. Using voltammetric and coulometric data, it can be concluded that the oxidation mechanism of caffeic acid (**1**) in the presence of *p*-toluenesulfinic acid, methyl-Meldrum's acid, and phenyl-Meldrum's acid is *EC*, and its oxidation mechanism in the presence of barbituric acid and Meldrum's acid is *ECEC*. ΔG_{tot} of caffeic acid and its substituted species were calculated, and the results indicate that ΔG_{tot} determines the direction of reactions.

2. EXPERIMENTAL SECTION

2.1. Apparatus and Reagents

Cyclic voltammetry experiments were conducted using an Ivium potentiostat/galvanostat (Netherlands) and a conventional three-electrode cell. A glassy carbon disk electrode (1.8 mm^2 surface area) was used as the working electrode, whereas a platinum wire served as the counter electrode. All potentials were measured versus an Ag/AgCl (3 M KCl) reference electrode. Controlled-potential coulometry experiments were performed using a BHP 2050

potentiostat/galvanostat (Iran) equipped with a digital coulometer. For controlled-potential coulometry, the working electrode consisted of an assembly of four carbon rods (1 cm diameter and 10 cm length), and a large platinum gauze was employed as the counter electrode. All electrodes were purchased from AZAR Electrode Co. (Iran). Caffeic acid, Meldrum's acid derivatives, *p*-toluenesulfinic acid, barbituric acid, and other chemicals were obtained from E. Merck and Aldrich and were used as received without further purification.

2.2. Computational details

The geometries of all possible structures were fully optimized in the gas phase at the standard 6-31G (d,p) basis set DFT (BP86) level of theory using Gaussian 09 [21]. Vibrational frequency analyses performed at the same theoretical level confirmed that all optimized structures correspond to stationary points on the potential energy surface, specifically local minima with no imaginary frequencies. Solvation energies were calculated using the Conductor-like Polarizable Continuum Model (CPCM) [22] with the ICOMP = 0 setting at the BP86 level of theory with the same basis set. Optimized atomic radii were employed via the solvent keyword RADII = UA0, and solvation free energies were obtained using the SCFVAC keyword.

3. RESULTS AND DISCUSSION

The electrochemical oxidation of caffeic acid (CA) was investigated in an aqueous solution using cyclic voltammetry at a glassy carbon (GC) electrode. The cyclic voltammogram (CV) of CA (**1**), recorded in an aqueous phosphate buffer solution (0.2 M, pH 2.1), is shown in Fig. 1. The CV exhibits a pair of anodic (A_1) and cathodic (C_1) peaks, corresponding to the oxidation of CA (**1**) to its o-benzoquinone form (**1ox**) and the subsequent reduction of **1ox** back to CA (**1**), respectively. This redox couple is attributed to a quasi-reversible two-electron, two-proton process [23]. As observed, the ratio of the cathodic to anodic peak currents (I_{pC1}/I_{pA1}) is approximately unity, indicating that under the experimental conditions the electrogenerated **1ox** species is stable at the electrode surface and does not undergo any follow-up chemical reaction after the electron transfer step.

The electrochemical oxidation of caffeic acid (**1**) in the presence of *p*-toluenesulfinic acid (*p*-TSA) as a nucleophile was investigated using cyclic voltammetry and controlled-potential coulometry. The cyclic voltammogram (Fig. 2, curve b) shows a decrease in the cathodic peak current (C_1) and the appearance of new redox peaks (A_2 and C_2) at more positive potentials. The reduction in I_{pC1} observed during the reverse scan indicates partial consumption of the electrochemically generated *o*-benzoquinone (**1ox**) through a follow-up chemical reaction with *p*-TSA (2) [24].

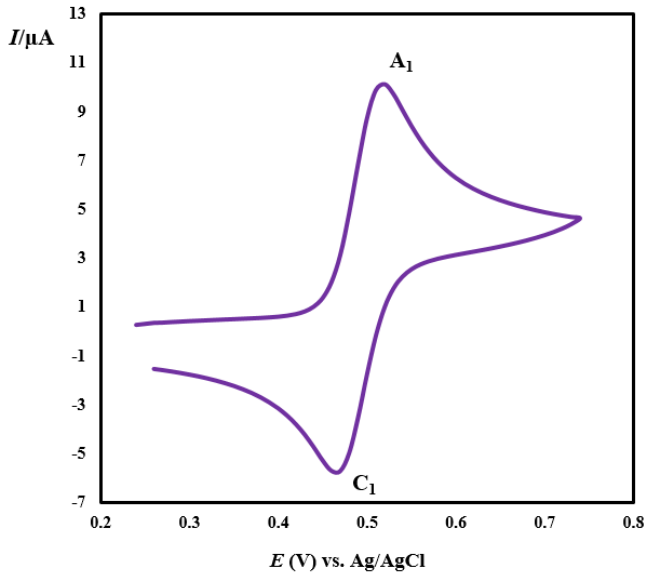

Figure 1. Cyclic voltammogram 1.0 mM of CA (**1**) at glassy carbon electrode, in phosphate buffer solution (c = 0.2 M, pH = 2.1); scan rate: 50 mV s^{-1}

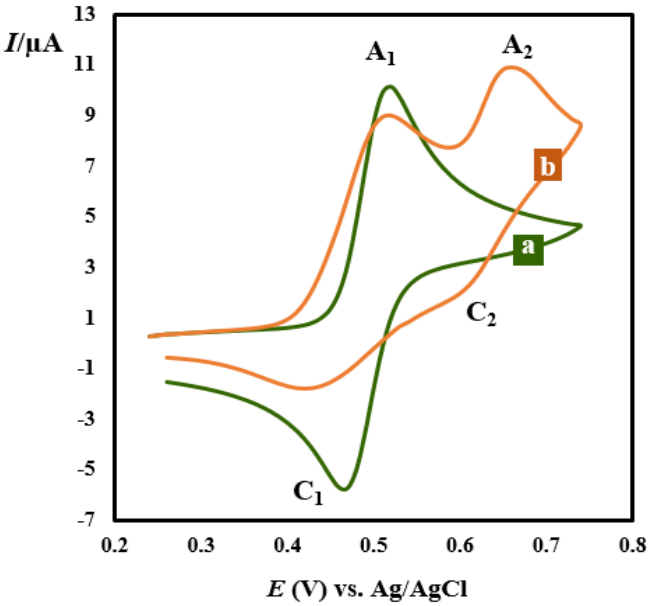

Figure 2. Cyclic voltammograms 1.0 mM of CA (**1**), *a*: in the absence, *b*: in the presence of 0.5 mM *p*-TSA (**2**) at a glassy carbon electrode in phosphate buffer solution (c = 0.2 M, pH = 2.1); scan rate: 50 mV s^{-1}

Further experiments performed at varying concentrations of *p*-TSA (2) showed that increasing the nucleophile concentration leads to: (a) a decrease in the peak current ratio I_{pC1}/I_{pA1}, consistent with the enhanced reactivity of the electrochemically generated o-benzoquinone (**1ox**) toward **2**; and (b) an increase in the ratio I_{pA2}/I_{pA1}, indicating the progressive formation of a secondary electroactive species [24].

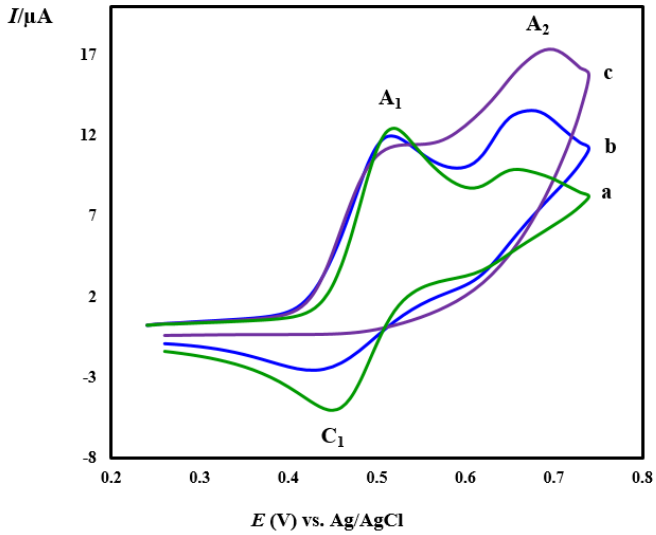

Figure 3. Cyclic voltammograms of 1.0 mM CA (**1**) in the presence of (*a*) 0.25, (*b*) 0.5 and (*c*) 1.0 mM *p*-TSA (**2**), at a glassy carbon electrode in phosphate buffer solution (pH 2.1, c = 0.2 M); Scan rate: 100 mV s^{-1}

It was observed that the scan rate has an inverse effect on the peak current ratio (I_{pC1}/I_{pA1}), with higher scan rates leading to an increase in this ratio. This behavior aligns with an *EC* mechanism, where faster scan rates reduce the time available for the chemical reaction between the electrochemically generated *o*-benzoquinone (**1ox**) and *p*-TSA(**2**), thereby preserving more **1ox** for reduction during the reverse scan. The appearance of a new pair of anodic (A_2) and cathodic (C_2) peaks at more positive potentials indicates the formation of an electroactive species with a higher oxidation potential than caffeic acid (**1**). Controlled-potential coulometry (CPC) was performed on an aqueous solution containing 0.25 mM caffeic acid (**1**) and 0.25 mM *p*-TSA (**2**) at 0.52 V vs. Ag/AgCl. Cyclic voltammograms recorded during electrolysis revealed that the process was halted when the charge consumption reached $2e^-$ per molecule of **1**. This observation, combined with prior studies on the electrochemical oxidation of **1** in the presence of different nucleophiles [27,28], supports the following pathway (Scheme 1): Electrochemical Step (*E*): CA (**1**) is oxidized to *o*-benzoquinone (**1ox**) via a two-electron process. Chemical Step (*C*): **1ox** reacts with *p*-TSA (**2**) to form a stable product (**2a**) that does not undergo further electrochemical oxidation under these conditions. According to Scheme 1, the anodic peaks A_1 and A_2 (Figure 2) correspond to the oxidation of caffeic acid (**1**) and intermediate **2a** to their respective *o*-benzoquinones (**1ox** and **2b**). The cathodic peaks C_1 and C_2 correspond to the two-electron reduction of *o*-benzoquinones **1ox** and **2b** to CA (**1**) and **2a**, respectively. Electrochemical oxidation of CA (**1**) in the presence of methyl-Meldrum's acid (MMA) and phenyl-Meldrum's acid (PMA) was studied using cyclic voltammetry and controlled-potential coulometry (CPC). The results indicate that the electrochemical oxidation mechanism of CA (**1**) in the presence of MMA (**3**) and PMA (**4**) is *EC* too (Scheme 2) [28].

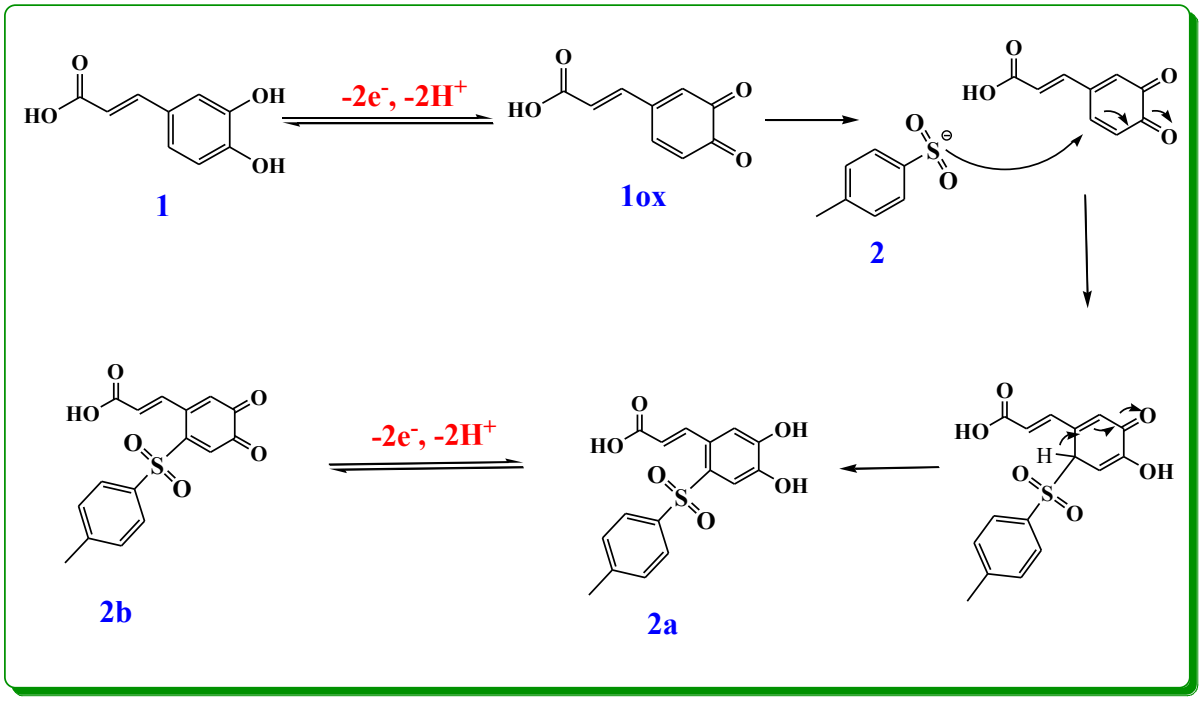

Scheme 1. Proposed mechanism for the electrochemical oxidation of caffeic acid (**1**) in the presence of *p*-TSA (**2**)

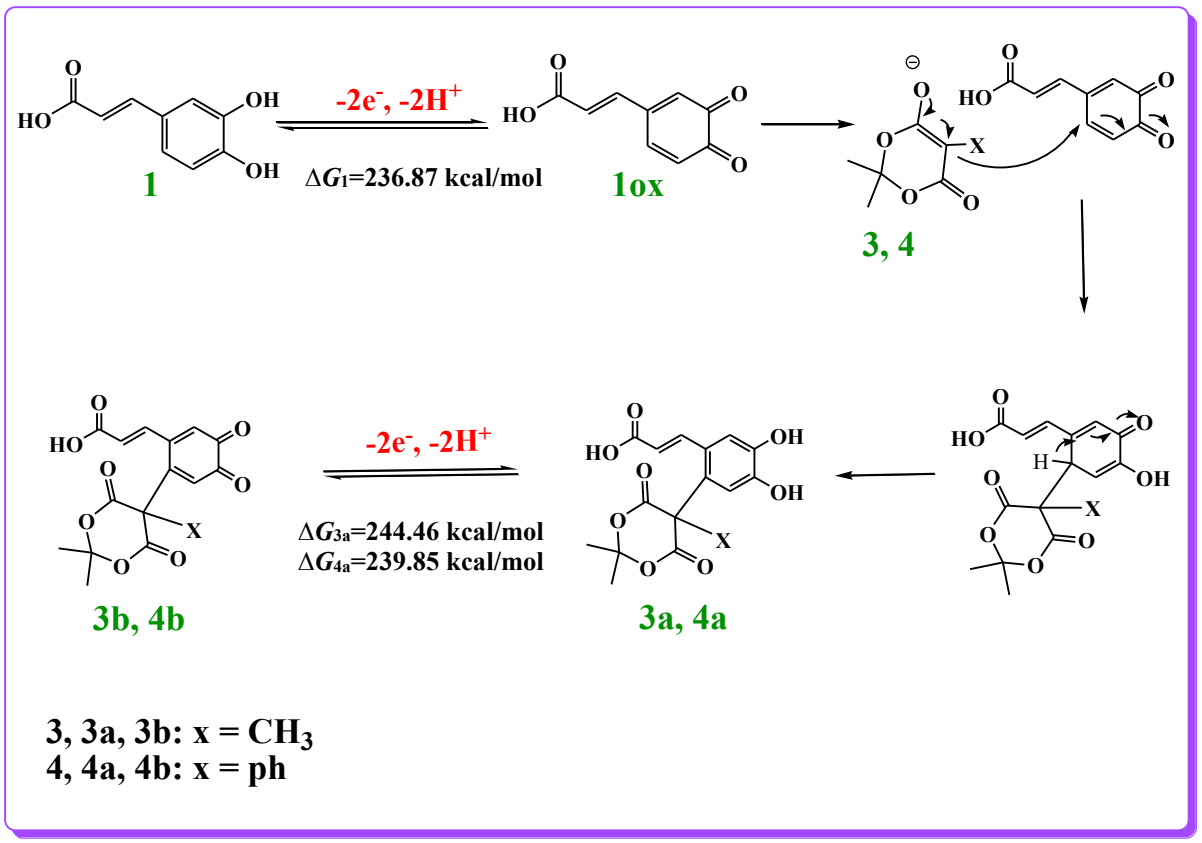

Scheme 2. Proposed mechanism for the electrochemical oxidation of caffeic acid (**1**) in the presence of methyl Meldrum's acid (**3**) and phenyl Meldrum's acid (**4**)

Our results indicate that the oxidation potentials of dihydroxybenzenes and their substituted species depend on the total change in Gibbs free energy (ΔG_{tot}) of the electrochemical oxidation, and it was observed that species with larger ΔG_{tot} value have more positive oxidation potential [18-20]. Since ΔG_{tot} influences the reaction mechanism, the ΔG_{tot} values of the studied compounds were calculated. The relationship between the oxidation potential and ΔG_{tot} is expressed as follows:

$$\Delta G_{tot} = -nF\,(E_C - E_A) \qquad (Eq.\ 1)$$

In this equation, E_A is the oxidation potential of the studied compounds. By considering the reduction of water as the cathodic reaction for all studied species, ΔG_{tot} is calculated using *E*q. 2.

$$\Delta G_{tot} = K + nFE_A \qquad (Eq.\ 2)$$

Where K is constant and ΔG_{tot} is the free energy change for the electrochemical oxidation of the studied species. As observed, ΔG_{tot} exhibits a linear relationship with E_A. The change in the Gibbs free energy, ΔG_{tot}, was calculated using 6-31G (p,d) basis set DFT(BP86) level of theory [15, 20, 29] based on the Born-Haber cycle (Figure 4) and *Eq*. 3.

$$\Delta G_{tot} = \Delta G^{redox}_{gas} + \Delta G^{redox}_{sol} \qquad (Eq.\ 3)$$

Where ΔG_{gas} is the standard Gibbs energy in the gas phase, and ΔG_{sol} is the solvation energy and is defined as follows:

$$\Delta G^{redox}_{gas} = \Delta G^{ox}_{sol} + 2\Delta G^{H+}_{sol} - \Delta G^{red}_{sol} \qquad (Eq.4)$$

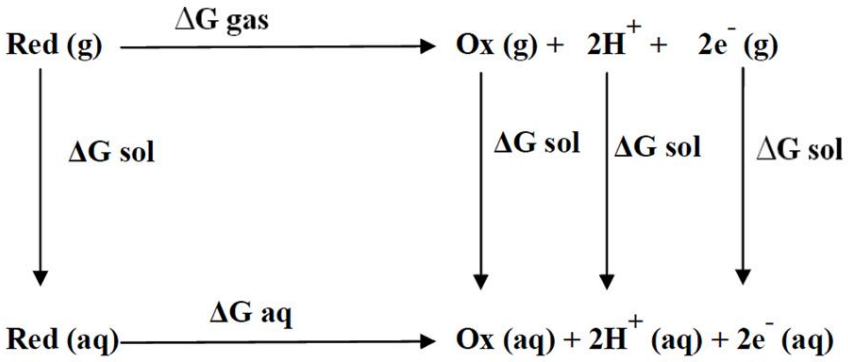

Figure 4. Thermodynamic cycle used to calculate Gibbs free energy

Based on *E*q. 2 it can be concluded that the larger the ΔG_{tot} of the species, the higher the value of the oxidation potential. In other words, if the ΔG_{tot} of a product is lower than that of the starting molecule, it can undergo oxidation during controlled-potential coulometry (CPC). Conversely, if the ΔG_{tot} of the product is higher than that of the starting molecule, it is not electroactive under CPC conditions, and the electrolysis terminates. The ΔG_{tot} values for the

electrochemical oxidation of **1** and **2a** were calculated. The results indicate that the ΔG_{tot} for the oxidation of **2a** is more positive than that of **1**, leading to an increased oxidation potential for **2a**. Consequently, the oxidation of **2a** is more difficult than that of the starting molecule **1**, and the final product (**2a**) is formed via an *EC* mechanism. The ΔG_{tot} values for the electrochemical oxidation of CA (**1**) in the presence of methyl-Meldrum's acid (MMA) and phenyl-Meldrum's acid (PMA) were calculated (Scheme 2). The results show that the ΔG_{tot} values for the oxidation of **3a** and **4a** are more positive than that of CA (**1**), corresponding to higher oxidation potentials. Therefore, the oxidation of **3a** and **4a** is more difficult than that of the starting molecule CA (**1**), and the final products are formed via an *EC* mechanism (Scheme 2).

The electrochemical oxidation of caffeic acid (CA, **1**) in the presence of barbituric acid (**5**) as a nucleophile was investigated using cyclic voltammetry, linear sweep voltammetry, and controlled-potential coulometry. Figure 5 presents the CVs of 1.0 mM CA (**1**) in an aqueous solution containing 0.2 M phosphate buffer (pH 6.0). As shown, the anodic peak current (A_1) increases, whereas the cathodic peak current (C_1) decreases in the presence of **5**.

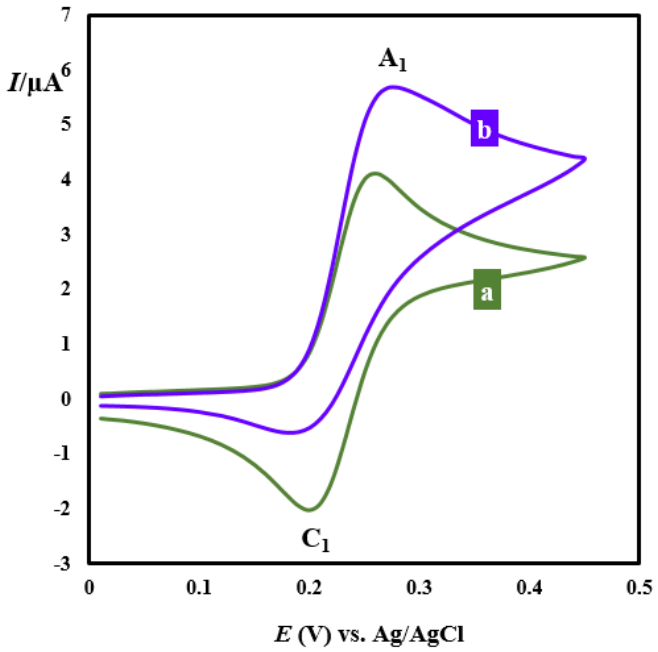

Figure 5. Cyclic voltammograms 1.0 mM of CA (**1**), *a*: in the absence, *b*: in the presence of 1.0 mM barbituric acid (**5**) at a glassy carbon electrode in phosphate buffer solution (c = 0.2 M, pH = 6.0); scan rate: 10 mV s^{-1}

Figure 6 illustrates the effect of potential sweep rate on the normalized linear sweep voltammograms (LSVs) of 1.0 mM CA (**1**) in the presence of 1.0 mM barbituric acid (**5**). The normalized voltammograms were obtained by dividing the current by the square root of the scan rate ($I/v^{1/2}$). As shown, the height of the normalized anodic peak (A_1) decreases

proportionally with increasing scan rate. Additionally, the effect of barbituric acid (**5**) concentration on the LSVs of CA (**1**) was investigated. The results indicate that the anodic peak current (A_1) increases with increasing concentrations of **5**. These electrochemical behaviors are attributed to the participation of the electrochemically generated *o*-quinone (**1ox**) in a subsequent chemical reaction with barbituric acid (**5**) [23].

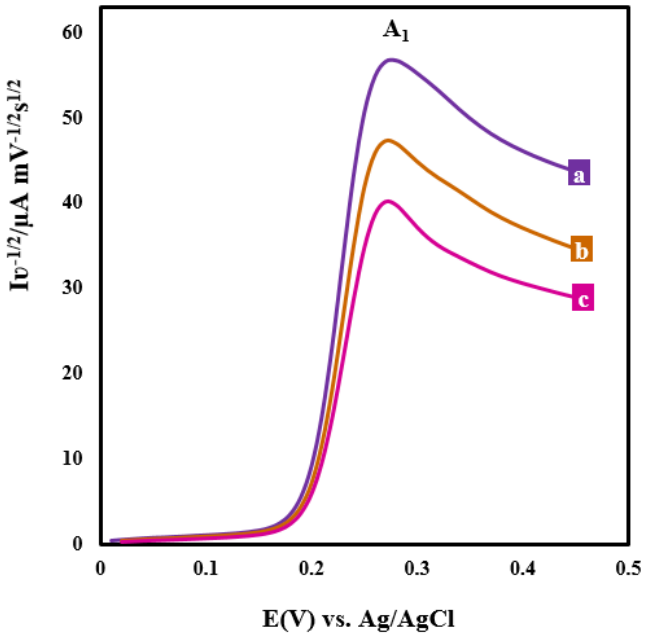

Figure 6. Normalized Linear-sweep voltammograms 1.0 mM of CA (**1**), in the presence of 1.0 mM barbituric acid (**5**) in phosphate buffer solution (pH 6.0) at various scan rates: (*a*) 10 mV s^{-1}, (*b*) 50 mV s^{-1} and (*c*) 100 mV s^{-1}

Controlled-potential coulometry (CPC) of 0.25 mmol CA (**1**) and 0.25 mmol barbituric acid (**5**) was performed in phosphate buffer (pH 6.0) at the potential of peak A_1 (0.27 V vs. Ag/AgCl). The progress of the electrolysis was monitored using cyclic voltammetry. The results indicate that as electrolysis proceeds, the anodic peak current (A_1) decreases and disappears when the charge consumption reaches approximately $4e^-$ per molecule of CA. The resulting product was characterized by ^{1}HNMR and ^{13}CNMR [23]. The voltammetric and coulometric data, together with previous studies on the electrochemical oxidation of CA in the presence of different nucleophiles [23,27,28], allow us to propose the pathway depicted in Scheme 3 for the oxidation of CA in the presence of barbituric acid (**5**). Scheme 3 shows that a Michael-type addition of **5** to the *o*-quinone (**1ox**) generates intermediate **5a**. Since the oxidation of **5a** is easier than that of **1**, **5a** is further oxidized to the corresponding *o*-quinone (**5b**). Subsequently, an intramolecular spirocyclization occurs, and the final product **5c** is formed via an *ECEC* mechanism. Thermodynamic calculations indicate that ΔG_{tot} follows the order $\Delta G_{5c} > \Delta G_1 > \Delta G_{5a}$. Therefore, the oxidation of intermediate **5a** is easier than that of CA

(**1**) or **5c**, which facilitates the oxidation of **5a** during CPC. In contrast, the ΔG_{tot} for the oxidation of **5c** is more positive than that of CA (**1**), corresponding to a higher oxidation potential. Consequently, the oxidation of **5c** is more difficult than that of CA, and the final product (**5c**) is formed via the *ECEC* mechanism.

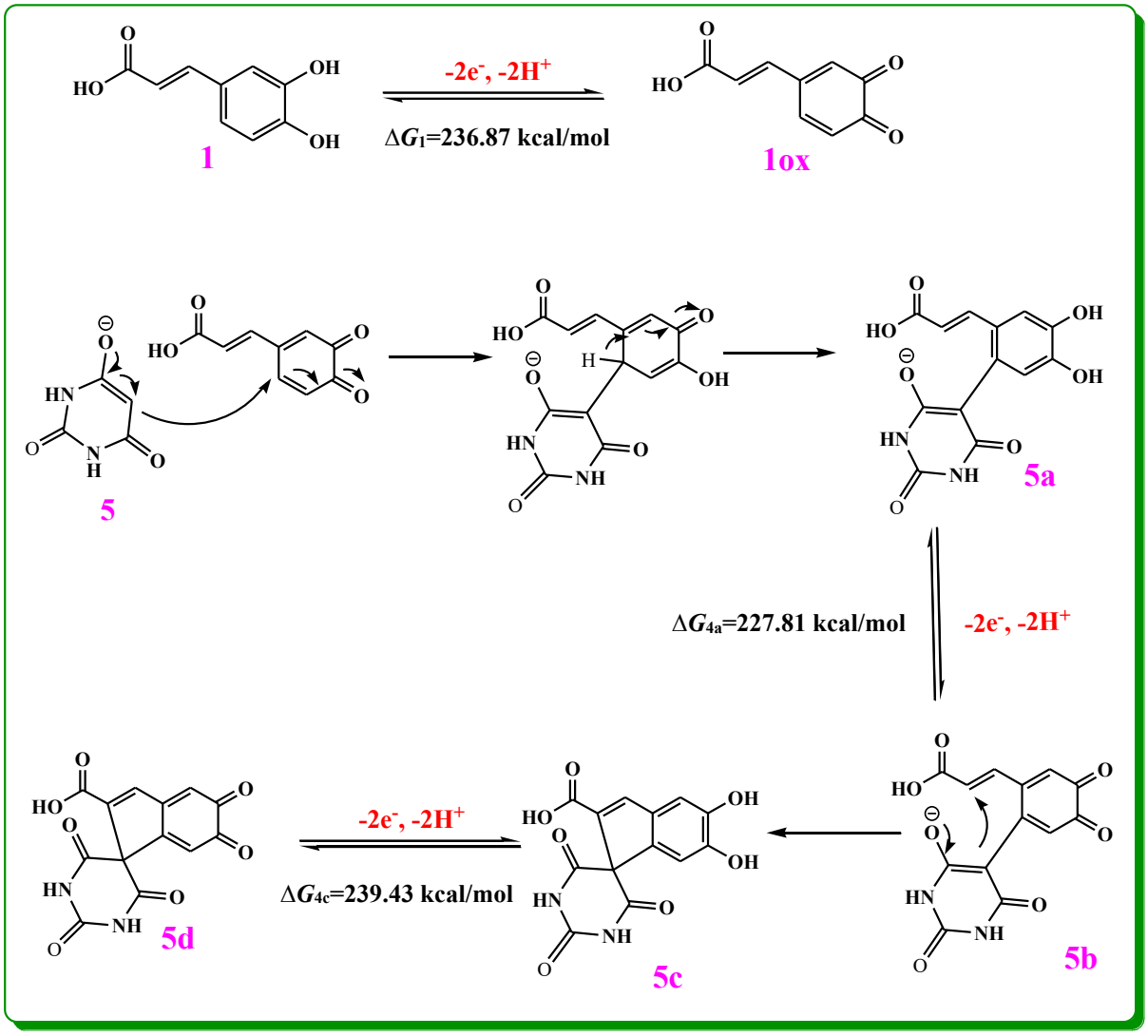

Scheme 3. Proposed mechanism for the electrochemical oxidation of caffeic acid (**1**) in the presence of barbituric acid (**5**)

The cyclic voltammogram of CA (**1**) in the presence of Meldrum's acid (**6**) as a nucleophile in an aqueous solution containing phosphate buffer (pH=6.0, c=0.2 M) is shown in Figure 7 (curve *b*). As shown in the presence of Meldrum's acid (**6**), the height of the anodic peak increased. The increase in the anodic peak current (A_1) indicates that the electrochemically generated *o*-benzoquinone (**1ox**) reacts with the nucleophile (**6**), producing a product that undergoes oxidation at the electrode surface, thereby amplifying the A_1 current.

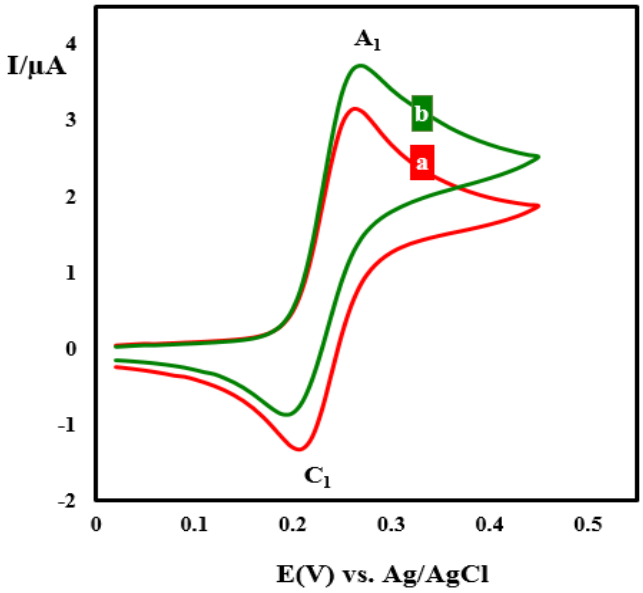

Figure 7. Cyclic voltammograms 1.0 mM of CA (**1**), *a*: in the absence, *b*: in the presence of 1.0 mM Meldrum's acid (**6**) at a glassy carbon electrode in phosphate buffer solution (c = 0.2M, pH = 6.0); scan rate: 5 mV s^{-1}

Figure 8 displays LSVs of caffeic acid (**1**) in the presence of varying concentrations of the nucleophile (**6**). As shown, the current of the anodic peak A_1 increases with increasing concentration of Meldrum's acid (**6**).

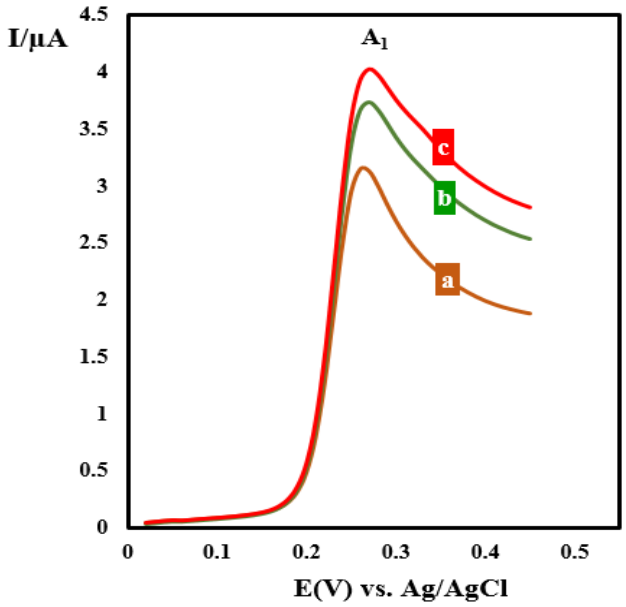

Figure 8. Linear-sweep voltammograms of 1.0 mM CA (**1**) in the presence of (*a*): 0 mM, (*b*) 1.0 mM, and (*c*) 2.0 mM of Meldrum's acid (**6**) at a glassy carbon electrode in phosphate buffer solution (c = 0.2 M, pH = 6.0); scan rate: 5 mV s^{-1}

This trend correlates with an enhanced homogeneous reaction rate for the subsequent chemical reaction between the electrochemically generated *o*-benzoquinone (**1ox**) and **6**, thereby amplifying the A_1 current. Also, the effect of potential scan rate on the electrochemical oxidation of caffeic acid (**1**) in the presence of Meldrum's acid (**6**) was investigated. The results indicated that the normalized current of the anodic peak A_1 decreases with increasing scan rate, which is attributed to the diminished contribution of the subsequent chemical reaction (coupling between **1ox** and **6**) at higher sweep rates.

Figure 9 shows the first and second cyclic voltammograms of 1 mM caffeic acid (**1**) in the presence of 2 mM Meldrum's acid (**6**). As the concentration of nucleophile (**6**) increases, a new anodic peak (A_2) emerges at more positive potentials. This observation raises a question: which species corresponds to the oxidation process at A_2? The appearance of A_2 suggests that a secondary species, generated at the electrode surface during the oxidation of **1**, undergoes oxidation at a higher potential than CA (**1**). A plausible explanation is that two species form at the electrode: *a*) A product that oxidizes at a potential similar to or slightly negative relative to CA (**1**), *b*) A secondary product that requires a higher overpotential for oxidation, generating the new A_2 peak.

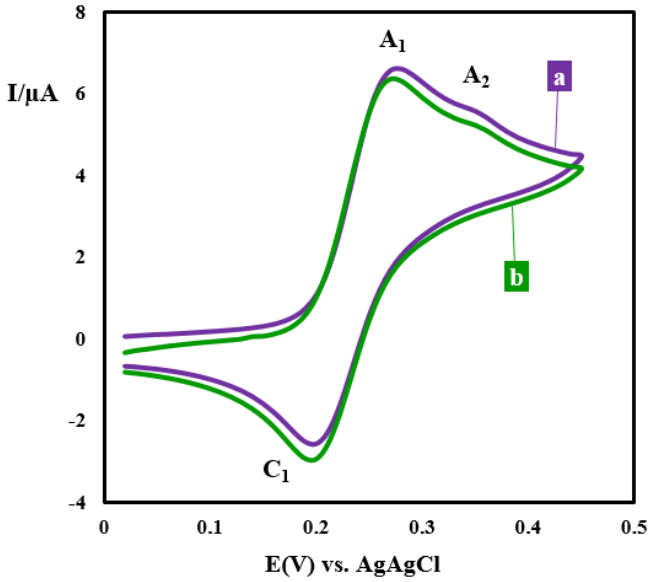

Figure 9. The first and the second cycle 1.0 mM of CVs of CA (**1**) in the presence 2.0 mM of Meldrum's acid (**6**) at a glassy carbon electrode, in phosphate buffer solution (pH 6.0); scan rate: 25 mV s^{-1}

To obtain more data, controlled-potential coulometry (CPC) was performed on a 60/40 (v/v) water/acetonitrile mixture containing phosphate buffer (pH 6.0), 0.3 mmol of caffeic acid (**1**), and 0.3 mmol of Meldrum's acid (**6**). Electrolysis was conducted at the potential of the A_1 peak (0.27 V vs. Ag/AgCl), and the reaction progress was monitored via cyclic voltammetry (Figure 10). The CVs recorded during CPC revealed a gradual decrease in the A_1 peak current

concurrent with charge consumption, until A_1 ultimately disappeared. The electrolysis was terminated when the charge consumption reached approximately $4e^-$ per molecule of **1**. At the endpoint, a pair of anodic (A_2) and cathodic (C_2) peaks remained. Voltammogram (e) in Figure 10 confirms the formation of an electroactive product that oxidizes at more positive potentials than the A_1 peak. The voltammetric data, the consumption of four electrons per molecule of caffeic acid (**1**) during controlled-potential coulometry (CPC), and prior mechanistic studies on the electrochemical oxidation of CA (**1**) with nucleophiles [23, 27, 28] collectively support the proposed mechanism for its oxidation in the presence of Meldrum's acid (**6**) (Scheme 4). Electrochemical Oxidation (E_1): **1** undergoes two-electron oxidation to form the *o*-quinone (**1ox**). Chemical Step (C_1): **1ox** undergoes a Michael addition with Meldrum's acid (**6**), yielding intermediate **6a**. Electrochemical Oxidation (E_2): **6a**, which is more readily oxidized than **1**, undergoes a second two-electron oxidation. Chemical Step (C_2): **6a** undergoes intramolecular spirocyclization, forming the final product **6b** via an *ECEC* pathway (Electrochemical → Chemical → Electrochemical → Chemical).

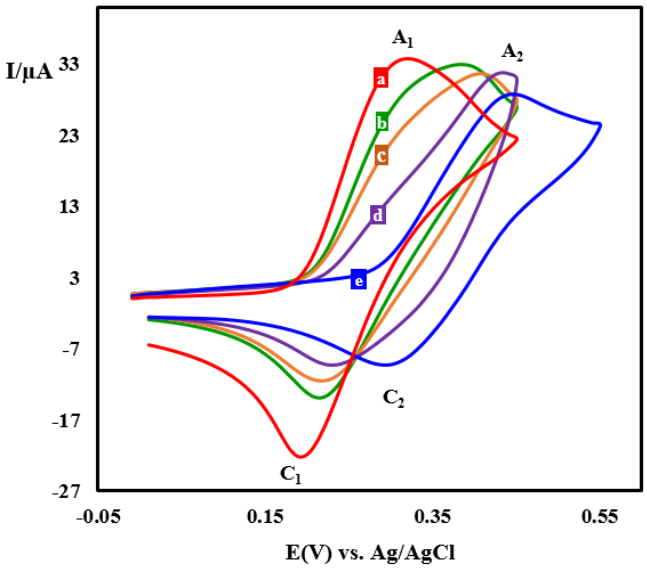

Figure 10. Cyclic voltammograms of CA (**1**) (0.30 mmol) in the presence of Meldrum's acid (**6**) (0.30 mmol) during controlled-potential coulometry at 0.27 V vs. Ag/AgCl in a 60/40 (v/v) water (phosphate buffer, pH 6.0)/acetonitrile mixture after the consumption of (a) 0 C, (b) 20 C, (c) 60 C, (d) 90 C, and (e) 110 C; scan rate = 100 mV s^{-1}

As shown in Scheme 4, the ΔG_{tot} of the electrochemical oxidation of CA (**1**), **6a** and **6c** were calculated. The results indicate that ΔG_{tot} varies in the order **6c** > **1**> **6a**. Because $\Delta G_{\mathbf{6a}}$ is less than $\Delta G_{\mathbf{1}}$, electrochemical oxidation of **6a** is easier than that of caffeic acid (**1**). Also the $\Delta G_{\mathbf{1}}$ is less than $\Delta G_{\mathbf{6c}}$, therefore, oxidation of **6c** is more difficult than the oxidation of CA (**1**).

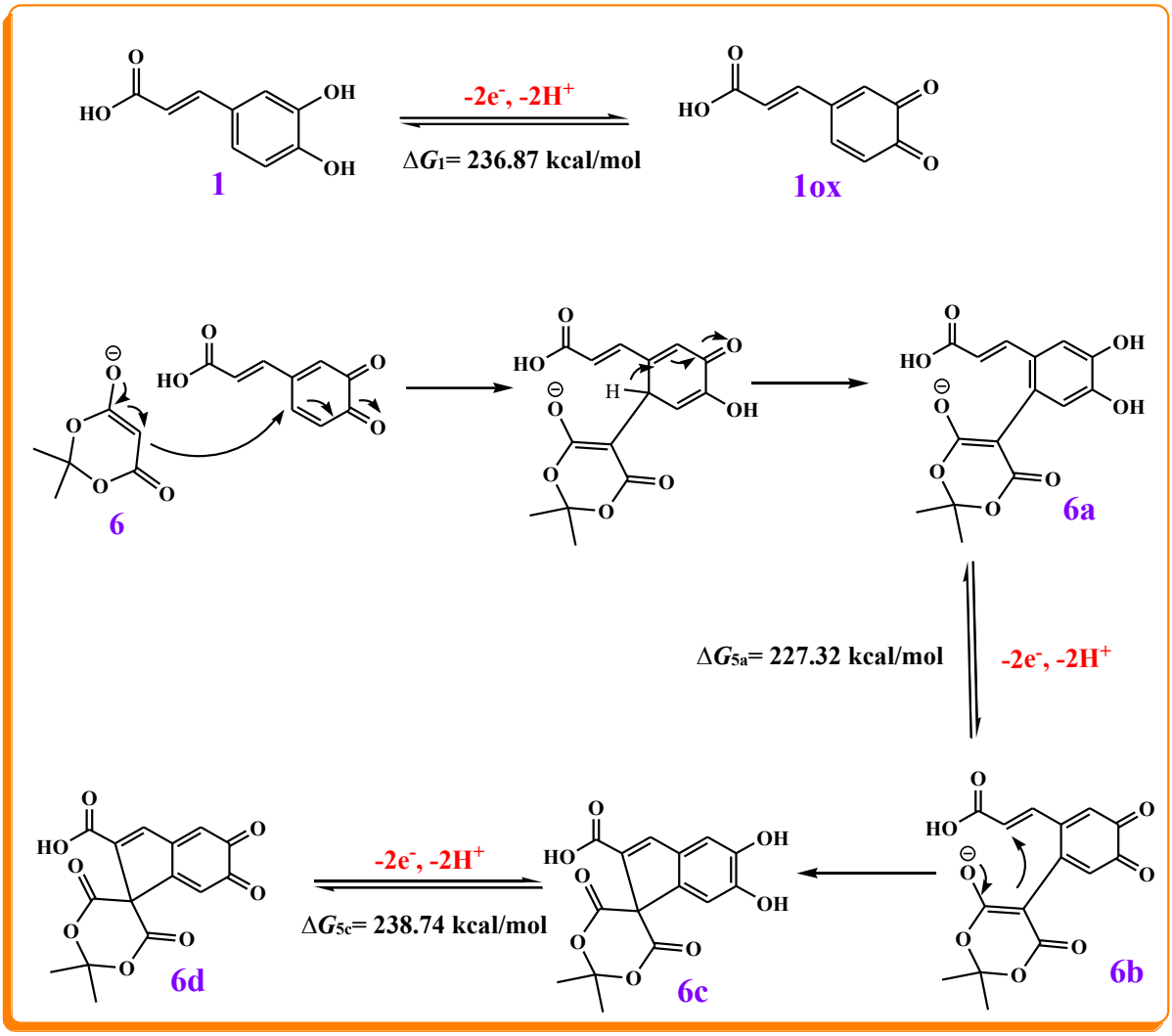

Scheme 4. Proposed mechanism for the electrochemical oxidation of caffeic acid (**1**) in the presence of Meldrum's acid (**6**)

For a better comparison, the ΔG_{tot} of the studied species were summarized in Table 1.

Table 1. ΔG_{tot} of the studied species

ΔG_{tot} (kcal/mol)	Species
236.78	**1**
246.12	**2a**
244.46	**3a**
239.85	**4a**
227.81	**5a**
239.43	**5c**
227.32	**6a**
238.74	**6c**

In other words, the oxidation potential varies in the order $E_{6c}>E_1>E_{6a}$ and consequently **6a** was produced as the final product via an *ECEC* mechanism. According to Scheme 4, the anodic peaks A_1 and A_2 (Fig. 10) correspond to the oxidation of CA (**1**) and **6c** to **1ox** and **6d**, respectively. In addition, the cathodic peaks C_1 and C_2 correspond to the reduction of **1ox** and **6d** to **1** and **6c**, respectively.

4. CONCLUSION

Cyclic voltammetry, linear sweep voltammetry, and controlled-potential coulometry indicate that the electrochemical oxidation of caffeic acid (1) in the presence of barbituric acid (5) and Meldrum's acid (6) follows an ECEC mechanism (Schemes 3 and 4). In contrast, the oxidation of caffeic acid in the presence of p-toluenesulfinic acid (2), methyl-Meldrum's acid (3), and phenyl-Meldrum's acid (4) proceeds via an EC mechanism (Schemes 1 and 2). Computational analyses of the reaction mechanisms revealed that when the ΔGtot of the product is lower than that of the starting species, the electrochemically generated intermediate can undergo further oxidation during controlled-potential coulometry. In other words, the difference in the anodic oxidation mechanism is related to the difference in the ΔGtot of the species

Acknowledgments

The authors acknowledge the Malayer University Research Council for supporting this work.

Declarations of interest

We confirm that this manuscript has been submitted exclusively to the Analytical & Bioanalytical Electrochemistry. This manuscript is not currently under consideration for publication elsewhere, and no portion of this material has been previously published in any medium including electronic journals or computer databases of a public nature. The authors declare no conflict of interest in this reported work.

REFERENCES

[1] J.F. Martinez-Suarez, J.A. Caram, G.A. Echeverria, O.E. Piro, A.M. Gennaro, and M.V. Mirifico, J. Org. Chem. 84 (2019) 6879.

[2] M. Rafiee, M.N. Mayer, B.T. Punchihewa, and M.R. Mumau, J. Org. Chem. 86 (2021) 15866.

[3] W. Zhao, Y. Lu, Y. Qiao, X. Yin, C. Liu, Z. Fang, J. Zhu, and K. Guo, Org. Lett. 25 (2023) 7451.

[4] M. Mehrdadian, S. Khazalpour, A. Amani, and M. Jamshidi, Electrochim. Acta 381 (2021) 138242.
[5] M. Jamshidi, D. Nematollahi, and H. Amiri-Rudbari, J. Electrochem. Soc. 163 (2016) G145.
[6] B. Batanero, M.J. Perez, and F. Barba J. Electroanal. Chem. 469 (1999) 201.
[7] M. Akbari, H. Shayani-Jam, M. R. Yaftian, and M. Parinejad, J. Electroanal. Chem. 827 (2018) 160.
[8] A. Amani, S. Khazalpour, and D. Nematollahi, J. Electroanal. Chem. 670 (2012) 36.
[9] A.R. Fakhari, D. Nematollahi, and A. Bayandori-Moghaddam, Electrochim. Acta 50 (2005) 5322.
[10] H. R. Zare, M. Namazian, and M.L. Coote, Electrochim. Acta 54 (2009) 5353.
[11] A. Amani, and D. Nematollahi J. Org. Chem. 77 (2012) 11302.
[12] D. Nematollahi, and E. Tammari, J. Org. Chem. 70 (2005) 7769.
[13] D. Nematollahi, and A. Amani, J. Electroanal. Chem. 651 (2011) 72.
[14] D. Nematollahi, and R. Rahchamani Tetrahedron Lett. 43 (2002) 147.
[15] S. Aslemarz, H. Beiginejad, and N. Pakravan, Monatsh. Fur. Chem. 150 (2019) 1433.
[16] D. Nematollahi, and H. Shayani-jam J. Org. Chem. 73 (2008) 3428.
[17] H. Beiginejad, M. Moradi, S. Paziresh, and H. Farahani, J. Electrochem. Soc. 165 (2018) H698.
[18] H. Beiginejad, D. Nematollahi, and S. Khazalpour J. Electrochem. Soc. 164 (2017) H946.
[19] H. Beiginejad, J. Electroanal. Chem. 825 (2018) 77.
[20] H. Beiginejad, A. Amani, D. Nematollahi, and S. Khazalpour, Electrochim. Acta 154 (2015) 235.
[21] M. J. Frisch, et al. Gaussian 09 (Revision A 01), Gaussian, Inc., Wallingford, CT (2009).
[22] V. Barone, and M. Cossi, J. Phys. Chem. A 102 (1998) 1995.
[23] N. Pakravan, H. Shayani-Jam, H. Beiginejad, H. Tavafi, and S. Paziresh J. Electroanal. Chem. 848 (2019) 113286.
[24] C. Zeng, C. Liu, J. Zeng, and R. Zhong, J. Electroanal. Chem. 608 (2007) 85.
[25] H. Beiginejad, Z. Rafiee, and M. Moradi, J. Iran. Chem. Soc. 17 (2020) 935.
[26] A.J. Bard, and L.R. Faulker, Electrochemical Methods, 2nd ed., Wiley, New York (2001).
[27] N. Pakravan, H. Beiginejad, and H. Shayani-Jam, J. Electroanal. Chem. 871 (2020) 114290.
[28] N. Pakravan, H. Shayani-Jam, H. Beiginejad, and H. Tavafi, J. Iran. Chem. Soc. 18 (2021) 2679.

[29] H. Beiginejad, D. Nematollahi, M. Bayat, F. Varmaghani, and A. Nazaripour, J. Electrochem. Soc. 160 (2013) H693.